PCCP

View Online
Dynamic Article Links

Cite this: *Phys. Chem. Chem. Phys.*, 2011, **13**, 4974–4979

www.rsc.org/pccp

PAPER

Hierarchical superstructure of alkylamine-coated ZnS nanoparticle assemblies†

Nataly Belman,[ab] Jacob N. Israelachvili,[cd] Youli Li,[d] Cyrus R. Safinya,[e] Vladimir Ezersky,[a] Alexander Rabkin,[ab] Olga Sima[ab] and Yuval Golan*[ab]

Received 26th June 2010, Accepted 21st January 2011
DOI: 10.1039/c0cp00999g

We describe methodology for producing highly uniform, ordered and reproducible superstructures of surfactant-coated ZnS nanorod and nanowire assemblies, and propose a predictive multiscale "packing model" for superstructure formation based on electron microscopy and powder X-ray diffraction data on the superstructure, as well as on individual components of the nanostructured system. The studied nanoparticles showed a hierarchical structure starting from the individual faceted ZnS inorganic cores, onto which the crystalline surfactant molecules are adsorbed, to the superstructure of the nanoparticle arrays. Our results point out the critical role of the surfactant headgroup and polarity in nanoparticle assembly, and demonstrate the relationship between the molecular structure of the surfactant and the resulting superstructure of the nanoparticle assemblies.

1. Introduction

Functional arrays of anisotropic nanoparticles with size-dependent physical properties are of considerable fundamental and technological interest. They are proposed as basic one-dimensional building blocks in nano-based structures and devices. In order to make practical devices, the nanofabrication technique should have the ability to synthesize nanostructures with specific size and shape into desired architectures.[1–10] Ordered semiconductor nanoparticle arrays are attracting increasing interest since they offer tunability of material properties not only *via* conventional shape and size-dependent quantum confinement effects, but also due to the effect of particle–particle interactions on various physical properties. Thus, it is important to identify the conditions under which nanoparticles assemble into two-dimensional (2D) and three-dimensional (3D) superstructures. Surfactant molecules are commonly used for controlling the size and shape of nanoparticles by specifically adsorbing onto various facets of the crystalline nanoparticles. However, the exact role of the surfactant in ordering nanoparticles into structured arrays has not been established.[11–15]

Zinc sulfide (ZnS) is a direct and wide band gap (3.91 eV) compound semiconductor that has a high index of refraction and high transmittance in the visible range and is an important material for photonic applications. Anisotropic ZnS nanoparticles are potentially useful in nanomaterial-based devices such as fluorescent displays, electroluminescent devices, infrared windows, lasers, solar cells and sensors.[3,4,16,17]

Structural characterization of surfactant-coated crystalline assemblies, using transmission electron microscopy (TEM) and X-ray diffraction (XRD) was previously studied by others.[18–20] Still, none of those studies have presented a multi-scale "packing model" that would describe the hierarchical assembly of nanoparticles into superstructures.

Octadecylamine (ODA, $C_{18}H_{37}NH_2$) surfactant is widely used as capping agent for nanoparticle synthesis.[6,7,16,21–31] We have recently showed that alkylamines (AAs) readily form alkylammonium-alkylcarbamate (AAAC) molecular pairs upon reaction with ambient carbon dioxide (CO_2).[28,32–36] Temperature-resolved powder XRD studies allowed to determine the structures of pure AAs and two phases of their AAAC analogs at room temperature and high temperature. In the case of octadecylammonium-octadecylcarbamate (OAOC), the high temperature structure was identified upon rapid heating of the OAOC to 92 °C.[28,36] After isolating the AAs and AAACs in pure form, the 3D structures of several AAs and AAACs[28,36] were deciphered and compared to the previously reported 2D structures of pure AA Langmuir films (LF) obtained at the air–aqueous solution interface.[16]

[a] *Department of Materials Engineering, Ben-Gurion University of the Negev, Beer-Sheva 84105, Israel. E-mail: ygolan@bgu.ac.il; Fax: +972-8-6472944; Tel: +972-8-6461474*
[b] *Ilse Katz Institute for Nanoscale Science and Technology, Ben-Gurion University of the Negev, Beer-Sheva 84105, Israel*
[c] *Department of Chemical Engineering, Materials Department, University of California, Santa Barbara, CA 93106, USA*
[d] *Materials Research Laboratory, University of California, Santa Barbara, CA 93106, USA*
[e] *Materials, Physics, and Molecular, Cellular, and Developmental Biology Departments, University of California, Santa Barbara, CA 93106, USA*

† Electronic supplementary information (ESI) available. See DOI: 10.1039/c0cp00999g

The AA-coated nanoparticles have been shown to assemble into ordered arrays in 2D and 3D, with spacings which can be varied by changing the surfactant chain length.[16,26,28,31] The formation of AA-coated ZnS nanorods and nanowires was previously reported by Pradhan *et al.*, and showed heterogeneous samples containing different morphologies of rods and wires in the same sample.[26] In the above mentioned synthetic protocols, AAs were used as received without further purification and no special storage conditions were mentioned. Hence, the AAs uncontrollably reacted with ambient CO_2, making it difficult to reproducibly obtain specific nanoparticle morphologies. We have shown that controlled exposure of AA to CO_2 prior to the synthesis allows control of the resulting nanoparticle morphology. Pure, unexposed AA results in nanowires, while controlled exposure of AA to CO_2 and partial AAAC formation results in nanorods.[28] *In situ* grazing incidence small-angle X-ray scattering (GISAXS) at the air–water interface was used for studying the 2D packing of AA-coated ZnS nanoparticle films and revealed the formation of superstructured nanoparticle arrays.[16]

In this work, we present new powder XRD data and integrate it with our previous understanding of the AA-ZnS system. This allowed us to solve the hierarchical superstructure of ODA-coated anisotropic nanorod and nanowire assemblies. The crystallographic orientation of the nanowires and nanorods was investigated with respect to the long axis of the nanoparticles using TEM. Based on those results, we present a multiscale "packing model" for superstructure formation, which ranges from the atomic level of the ZnS nanoparticle cores, through the mesostructure of the alkylamine surfactant molecules, to the superstructure formed by the composite organic-inorganic nanorods and nanowires. While in this article we give attention to nanoparticles coated with ODA (18 carbon) surfactant, the results were qualitatively similar upon using AAs with chain lengths of 14 and 16 carbons (not shown). Furthermore, the proposed model could provide insight on other surfactant-coated nanoparticle superstructures.

2. Experimental details

2.1 Materials

ODA (Fluka, 99%), potassium ethyl xanthogenate (Fluka, > 98%), zinc perchlorate hexahydrate (Aldrich, 96%) were used as received. The ODA was stored under argon at

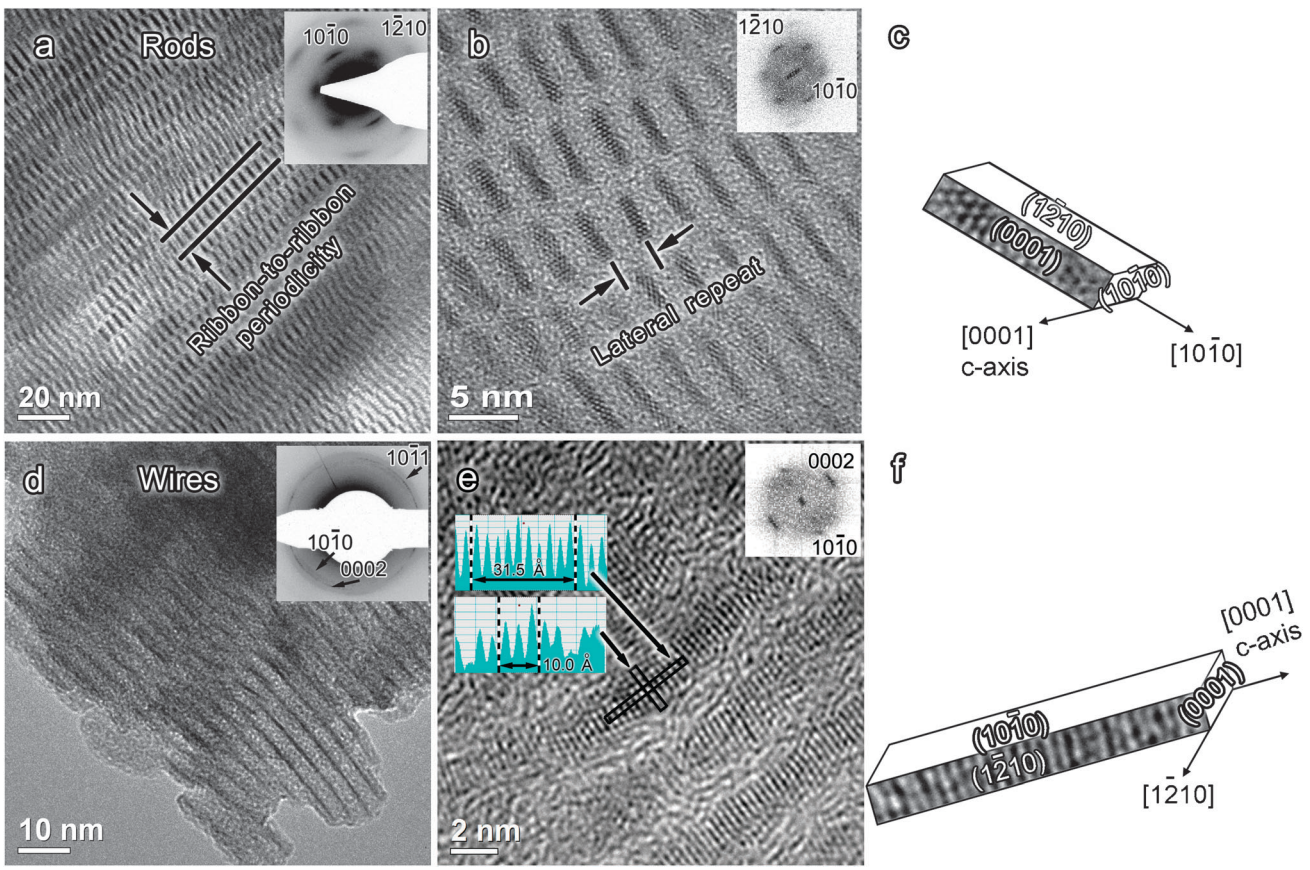

Fig. 1 (a) BF TEM image and ED pattern (inset) of ODA-coated ZnS nanorods. (b) HRTEM image of ZnS nanorods with FFT pattern (inset). Ribbon-to-ribbon and lateral repeat periodicity are denoted in (a) and (b), respectively. (c) Schematic representation of planes and directions within an individual ODA-coated ZnS nanorod. (d) BF TEM image and ED pattern (inset) of ODA-coated ZnS nanowires. (e) HRTEM image of ZnS nanowires with FFT pattern and intensity periods indicating the 3.15 and 3.33 Å d-spacings observed in the image (insets). (f) Schematic representation of planes and directions within an individual ODA-coated ZnS nanowire. Note the different orientation of the rods and wires with respect to the long axis of the rod/wire.

all times. Methanol (Gadot, absolute) and chloroform (Frutarom, CP) were used for all experiments. Deionized water used for synthesis (resistivity 18.2 MΩ cm) was obtained from a Millipore filter system.

2.2 Nanoparticle preparation

Zinc-ethylxanthate ($Zn(SSCOC_2H_5)_2$) was prepared by dissolving 3.00 g of potassium ethyl xanthogenate and separately 3.48 g of zinc perchlorate hexahydrate in water. The solutions were mixed together and zinc xanthate salt precipitated out. The salt was washed 5 times with water, filtered and dried in air. ODA-coated ZnS nanoparticles were prepared using a modified synthesis based on the method of Pradhan *et al.*[26] 0.08 g of zinc-ethylxanthate was dissolved in 1.53 g of molten ODA. The reaction was carried out in a glass test tube immersed in hot silicone oil with nitrogen purged into the test tube. The addition of zinc xanthate powder to molten surfactant resulted in a yellowish-white hazy solution and almost immediately a white turbidity appeared, indicating the formation of ZnS. The ODA-coated ZnS nanoparticles were harvested by flocculating the sample with methanol, separating by centrifugation, redispersing in chloroform and drying in air. The typical mass of a batch of dried ODA-coated nanoparticles was 0.2 ± 0.1 g. For nanowire formation, *pure unexposed* ODA was used. The nanowires can be synthesized in a two-step reaction: nucleation at 105–120 °C for 5 min and then the reaction is held at 130–150 °C for an additional 8–60 min. In this work, nanowires were synthesized using the following two-step reaction: nucleation at 110 °C for 5 min, followed by additional 60 min at 130 °C for. For nanorod synthesis ODA is initially *exposed to* CO_2 to form OAOC (ODA mass gain 2–5 wt%).[28] In this work, the nanorods were prepared by controllably exposing ODA to ambient air until ODA mass gain was 4.5 wt%. The nanorod synthesis was carried out in a two-step reaction: 105 °C for 5 min, and then an additional 8 min at 130 °C.

2.3 Characterization methods

Powder XRD characterization of ODA-coated nanoparticles was carried out using a custom built wide angle X-ray scattering (WAXS) diffractometer equipped with a Rigaku UltraX18 rotating anode generator (Cu-Kα, λ = 1.54 Å), an OSMIC double-focusing multilayer monochromator and a MAR345 image plate detector. The powder samples were placed into 1.5 mm diameter quartz capillaries.

TEM analyses were carried out using a Tecnai G^2 TEM operating at 120 kV and JEOL 2010 Fas-TEM equipped with a UHR pole piece operating at 200 keV. The samples were prepared by placing a droplet of a chloroform suspension of the nanoparticles on a lacey carbon-coated TEM grid (400 mesh, SPI 3840C-MB) and dried in ambient air.

3. Results and discussion

In order to understand the parameters that affect the assembly of the ODA-coated ZnS nanoparticles into superstructures, samples were analyzed using complementary TEM and XRD techniques. The above structural studies were coupled with the comprehension we have previously gained of the structure, reactivity and phase transition upon heating of the ODA surfactant.[28,36] Ordered arrays of ODA-coated ZnS nanorods and nanowires were prepared using a modified synthesis based on the method of Pradhan *et al*. For the nanorods, ODA was controllably exposed to the ambient air such that ODA mass gain was 4.5 wt% due to reaction with the ambient CO_2 and OAOC formation (see the Experimental details section above).[26,28] Bright field (BF) TEM images of ODA-coated ZnS nanoparticles with narrow width distribution of 10 ± 2 Å are shown in Fig. 1. The nanorods, 50 ± 10 Å long, assembled into highly ordered 2D super-crystalline arrays which were stacked in "ribbon-like" columns (Fig. 1a). The ribbon-to-ribbon periodicity (marked in Fig. 1a) was 72 ± 2 Å and within each ribbon the ZnS nanorods were separated by a well-defined lateral repeat of 37 ± 2 Å (marked in the high resolution TEM (HRTEM) lattice image in Fig. 1b). The electron diffraction (ED) pattern of the ZnS core in Fig. 1a (inset) indicates interplanar spacings of $d_{10\bar{1}0}$ = 3.30 ± 0.07 Å and $d_{1\bar{2}10}$ = 1.92 ± 0.03 Å, very close to the Joint Committee on Powder Diffraction Standards (JCPDS) file values of $d_{10\bar{1}0}$ = 3.310 Å and $d_{1\bar{2}10}$ = 1.910 Å for wurtzite ZnS.[37] The diffraction pattern corresponds to the [0001] zone axis (growth along the $10\bar{1}0$ crystallographic direction), which is rather unusual since in wurtzite crystals growth rate is normally fastest along the *c*-axis.[38] The zone axis was confirmed by HRTEM. A HRTEM image of the nanorods is shown in Fig. 1b. The hexagonal lattice image is characteristic of the [0001] orientation, as shown in the FFT analysis (inset).

Nanowires with lengths varying from 100 to thousands of Å and lateral interparticle spacing of 38 ± 3 Å are shown in TEM images in Fig. 1d,e. For nanowire formation, pure unexposed ODA was used (see the Experimental details section above). The large area ED pattern in Fig. 1d (inset) indicates a wurtzite structure of the ZnS core, with two very weak $d_{10\bar{1}0}$ = 3.32 ± 0.04 Å and $d_{10\bar{1}1}$ = 2.90 ± 0.04 Å and one strong d_{0002} = 3.07 ± 0.06 Å reflections, close to the JCPDS values of $d_{10\bar{1}0}$ = 3.32 Å, d_{0002} = 3.13 Å and $d_{10\bar{1}1}$ = 2.926 Å.[37] The ED pattern indicates that the [0001] direction (*c*-axis) is parallel to the long axis of the wire. The zone axis could not be identified from the ED pattern, since it was taken from a large area of wires, forming a "powder" pattern of rings. In order to determine the zone axis, HRTEM was performed. A HRTEM lattice image of the nanowires is shown in Fig. 1e. The interplanar distances, calculated using intensity periods of the HRTEM image (Fig. 1e, inset) were 3.15 and 3.33 Å, corresponding to the (0002) planes normal and ($10\bar{1}0$) planes parallel to the long axis of the wire. The FFT analysis (Fig. 1e, inset) confirmed the [$1\bar{2}10$] orientation of the wires with respect to the electron beam. Schematic representations of an individual nanorod and an individual nanowire, indicating the planes and directions based on the TEM results, are shown in Fig. 1c and f, respectively.

Formation of two different nanoparticle morphologies might be related to the phase transition occurring in OAOC upon heating.[28,36] We have detected, using a control experiment, that during the nanorod synthesis all CO_2 is released from the surfactant. Nevertheless, the development of nanorod morphology may be associated with the formation of the high temperature phase of OAOC at 92 °C [28,36] and hence, the

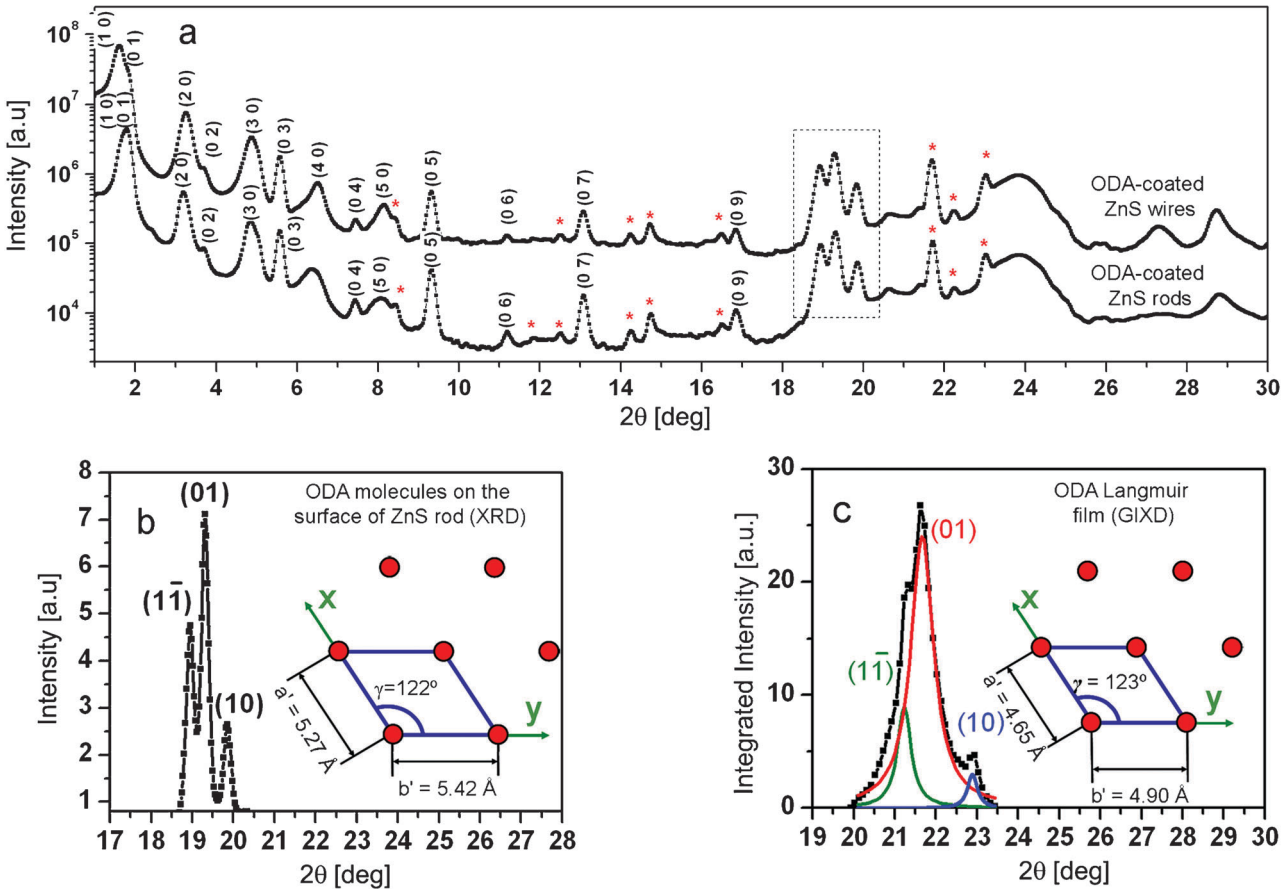

Fig. 2 (a) Powder XRD patterns and Bragg peak indexing of ODA-coated ZnS nanorods and nanowires. Several peaks in the diffractograms (marked with *) are correlated to OAOC surfactant powder,[28,36] indicating the presence of a small amount of excess free surfactant. The dashed rectangle denotes the in-plane peaks of the surfactant. (b) Magnified section of an XRD pattern showing the Bragg peaks of ODA-coated ZnS nanorods, marked with a dashed rectangle in (a). (c) Deconvoluted projection of the GIXD-measured intensity onto the $2\theta_{xy}$ axis, and Bragg peak indexing for an ODA Langmuir film.[16] Insets in (b) and (c) schematically represent top views of the oblique 2D unit cells of ODA molecules on the facetted surface of ZnS rods, and at the air–aqueous solution interface,[16] respectively.

molecular arrangement of the surfactant during the nanorod synthesis is different from that of the pure ODA in the nanowire synthesis (pure ODA melts at 55 °C and does not form the high temperature phase).[36] Additionally, using pure ODA surfactant under the same synthesis conditions (temperature and duration) as described in the Experimental details section for the nanorod formation, resulted in formation of small domains of nanowires (Fig. S1 in Supplementary Information†). This confirms our conclusion that controlled exposure of the ODA to CO_2 is required for obtaining the nanorod morphology.

Electron microscopy provided information only on the ZnS core, and could not probe the structure of the surfactant molecules. For this purpose XRD measurements were carried out on powder samples of ODA-coated ZnS nanorods and nanowires (Fig. 2a). Note that peaks from the ZnS core were not observed in the XRD patterns in Fig. 2a, as was the case of anisotropic AA-coated ZnS nanoparticles investigated using synchrotron diffraction.[16] The absence of mineral peaks is explained by considerable peak broadening related to the ultra-small dimensions of the nanoparticles and due to the strong surfactant peaks. A magnified portion of the powder diffractogram is given in Fig. S2† together with the position of the mineral peaks as reported in the literature, which confirms the conclusion that the ZnS peaks cannot be observed using the XRD technique. Hence, it was established

Table 1 2D rectangular unit cell dimensions of the superstructure of lamellar ODA-coated nanoparticles, and 2D oblique unit cell dimensions of the ODA molecules arranged on the nanoparticle surface, as derived from powder XRD measurements (Fig. 2a). The error in the calculated lattice constants was ± 0.04 Å

	2D unit cell of lamellar ODA-coated nanoparticle superstructures		2D unit cell of the ODA on nanoparticle surface		
	a (Å)	b (Å)	a' (Å)	b' (Å)	γ (°)
ODA-coated wires	54.04	47.50	5.43	5.28	122.16
ODA-coated rods	54.75	47.49	5.42	5.27	122.08

that all the peaks in the XRD patterns in Fig. 2a correspond to the organic surfactant. Notably, several peaks in the nanoparticle diffractograms were observed also in the diffractograms obtained for the respective OAOC powder (marked with red asterisks), indicating the presence of a small amount of excess free surfactant in the samples. As expected, the excess surfactant is OAOC and not ODA due to nanoparticle drying conditions which allow for spontaneous absorption of CO_2 from ambient air.[28,36] Attempts to index the surfactant peaks did not yield a meaningful 3D unit cell solution, suggesting that the material is ordered in 2D and stacked in a complex hierarchical 3D packing. The lamellar ordering of the molecules is evident from the set of (*l*0) and (0*l*) spacings. The peaks were indexed to a 2D rectangular unit cell and the (*hk*) Miller indices are noted above each peak in Fig. 2a. The 2D lattice constants *a* and *b* are summarized in Table 1 and the indexed (*hk*) planes with the corresponding experimental and calculated d_{hk}-spacings are listed in Supplementary Table S1†.

For both XRD curves in Fig. 2a, three in-plane peaks were observed at the same position (marked by a dashed rectangle). For instance, the relevant section of the XRD pattern obtained for ODA-coated ZnS nanorods is shown in Fig. 2b. The peak positions are familiar to us from our previous grazing incidence X-ray diffraction (GIXD) studies of ODA LF at the air-aqueous solution interface (Fig. 2c), which indicated an oblique unit cell with lattice parameters $a' = 4.90$ Å, $b' = 4.65$ Å and $\gamma = 123°$ (inset in Fig. 2c).[16] Similarly, the (*hk*) Miller indices are noted above the peaks in the XRD pattern in Fig. 2b and the oblique 2D unit cell of ODA molecules on the surface of ZnS rods is schematically represented in the inset in Fig. 2b. The lattice constants a', b' and γ of the 2D arrangement of ODA molecules on the nanoparticle surface are summarized in Table 1 and the indexed (*hk*) planes with corresponding d_{hk}-spacings are listed in Supplementary Table S2.† Consequently, the XRD patterns of ODA-coated nanoparticles show peaks arising from two different sources: (i) 2D lamellar superstructure of ODA-coated nanoparticles giving rise to a set of high order lamellar peaks and (ii) in-plane 2D arrangement of ODA molecules within the lamellae on the nanoparticle surface. The corresponding area per ODA molecule on the faceted nanoparticle surface, calculated from the unit cell dimensions (inset in Fig. 2b) is 24.2 Å^2. This value is larger than the GIXD-measured area per ODA molecule at the air-aqueous solution interface (19.2 Å^2),[16] and than the cross sectional area of a hydrocarbon chain (~20.8 Å^2),[39] indicating that the molecules are less close-packed. The highly ordered nature of the ODA molecules bound to the ZnS nanoparticles and the similarity to the structure of ODA monolayers strongly suggests that the nanoparticles are *faceted*. This is since it is rather unlikely that the surfactant would crystallize in the same "natural" structure on such highly curved surfaces (with radius of curvature $r = 5$ Å). Schematic representations of the ZnS planes and directions within ODA-coated ZnS nanorods and nanowires are shown in Fig. 1c,f.

The following example is shown to demonstrate packing model of the ODA-coated nanorods, while the model is similar in case of nanowires. A schematic illustration depicting the 2D unit cell formed by ODA-coated ZnS nanorods, as derived from powder XRD, is shown in Fig. 3a. Notably, the above unit cell is consistent with the TEM data, since the 37 Å interparticle repeat distance observed by TEM (Fig. 1a,b; schematically shown in Fig. 3b) corresponds to the $d_{11} = 35.9$ Å spacing of the superstructure. Consequently, the green arrow in Fig. 3a represents the TEM-viewing direction. The illustration in Fig. 3a depicts one single 2D sheet of the nanorod assembly. The 3D multilayer structure is formed by stacking these 2D sheets (their projections are seen in the TEM images as "ribbons" of aligned nanorods; see Fig. 1a). The agreement between the spacings obtained in TEM and XRD confirms the 2D crystalline structure of the assembly. The thickness of the nanorods *t* could not be obtained from TEM (see Fig. 3a; this dimension is aligned parallel to the TEM

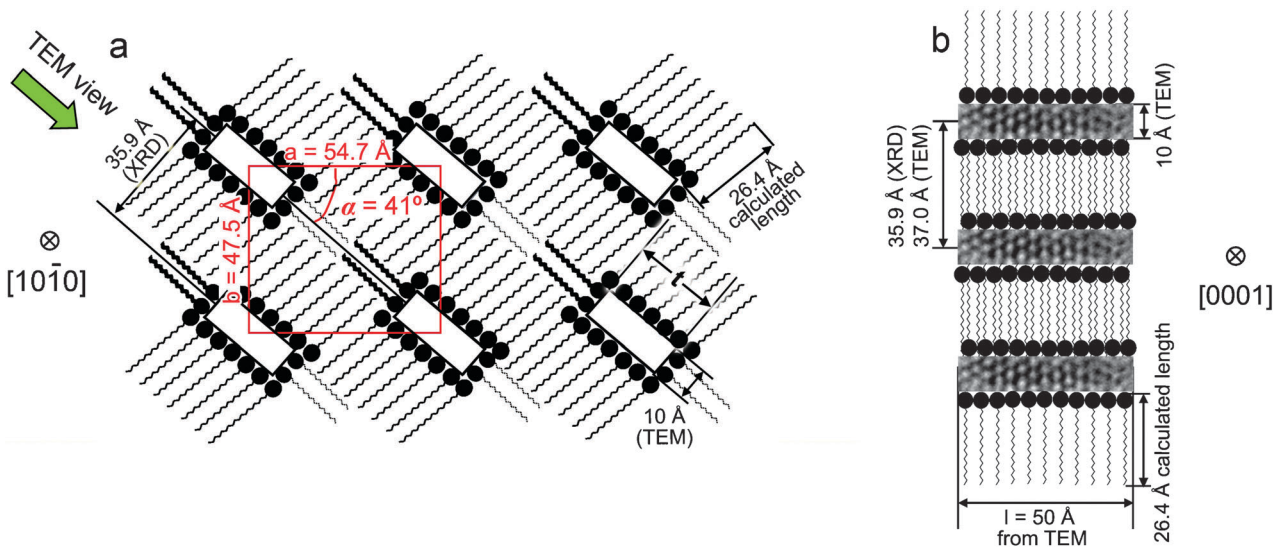

Fig. 3 (a) Schematic illustration of a tentative packing model of ODA-coated ZnS nanorods, viewed along the $[10\bar{1}0]_{ZnS}$ direction. The red rectangle outlines the 2D unit cell, as derived from XRD. The TEM image (see Fig. 1a,b) is viewed from the side, along the [11] direction of the superstructure (marked with a green arrow). (b) Corresponding illustration of the TEM view of ODA-coated ZnS nanorods (Fig. 1a,b) viewed along the [11] direction of the superstructure (see green arrow in (a)), namely, parallel to the $[0001]_{ZnS}$ direction.

electron beam), and was set in the packing model to ~25 Å in order to minimize unfavorable interactions between the hydrophobic tails and hydrophilic heads of the surfactants. The surfactants are likely to be arranged primarily as bilayers, similar to their native structure in the absence of the nanorods.[28,36]

Conclusions

Our study demonstrates that ODA-coated ZnS nanoparticles assemble into a layered superstructure that is clearly templated by the surfactant coating. The hierarchical structure starts from the uniform and highly aligned wurtzite ZnS cores, follows to the mesoscopic 2D in-plane structure of the surfactant molecules adsorbed onto the nano-sized ZnS facets, and finally, to the composite bilayer/nanorod assembly within 3D stacked sheets. As no correlation was observed in XRD and in TEM for the dimension perpendicular to the ordered sheets, they are likely to be stacked like a smectic liquid crystal, whose layers are seen as "ribbons" in Fig. 1a. Our findings point out the critical role of the surfactant head group and polarity in nanoparticle assembly, and demonstrate the relationship between the molecular structure of the surfactant and the resulting superstructure of the nanoparticle assemblies.

Acknowledgements

The help of D. Mogilyanski, J. Irwin and H. Schollmeyer with XRD is gratefully acknowledged. This work was supported by the US-Israel Binational Science Foundation, Grant #2006032 (JI and YG) and DOE-BES grant DE-FG02-06ER46314 (CRS and YL, X-ray nanoparticle structure), NSF grant DMR-0803103 (CRS). This work made use of MRL Central Facilities supported by the MRSEC Program of the National Science Foundation under award No. DMR05-20415.

References

1 O. D. Velev and S. Gupta, *Adv. Mater.*, 2009, **21**, 1897–1905.
2 I. Lisieckia and M. P. Pileni, *C. R. Chim.*, 2009, **12**, 235–246.
3 D. Moore, C. Ronning, C. Ma and Z. L. Wang, *Chem. Phys. Lett.*, 2004, **385**, 8–11.
4 Z. Wang, L. L. Daemen, Y. Zhao, C. S. Zha, R. T. Douns, X. Wang, Z. L. Wang and R. J. Hemley, *Nat. Mater.*, 2005, **4**, 922–927.
5 Z. M. Wang, *One-dimensional nanostructures*, Springer, Fayetteville, 2008.
6 S. Acharya, U. K. Gautam, T. Sasaki, Y. Bando, Y. Golan and K. Ariga, *J. Am. Chem. Soc.*, 2008, **130**, 4594–4595.
7 Q. Ji, S. Acharya, J. P. Hill, G. J. Richards and K. Ariga, *Adv. Mater.*, 2008, **20**, 4027–4032.
8 M. P. Pileni, *Acc. Chem. Res.*, 2008, **41**, 1799–1809.
9 M. Ghosh, F. Fan and K. J. Stebe, *Langmuir*, 2007, **23**, 2180–2183.
10 S. Acharya, J. P. Hill and K. Ariga, *Adv. Mater.*, 2009, **21**, 2959–2981.
11 S. Acharya, A. B. Panda, S. Efrima and Y. Golan, *Adv. Mater.*, 2007, **19**, 1105–1108.
12 A. M. Morales and C. M. Lieber, *Science*, 1998, **279**, 208–211.
13 I. Patla, S. Acharya, L. Zeiri, J. Israelachvili, S. Efrima and Y. Golan, *Nano Lett.*, 2007, **7**, 1459–1462.
14 H. Y. Peng, X. T. Zhou, N. Wang, Y. F. Zheng, L. S. Liao, W. S. Shi, C. S. Lee and S. T. Lee, *Chem. Phys. Lett.*, 2000, **327**, 263–270.
15 Y. Wu, B. Messer and P. Yang, *Adv. Mater.*, 2001, **13**, 1487–1489.
16 N. Belman, S. Acharya, O. Konovalov, A. Vorobiev, J. Israelachvili, S. Efrima and Y. Golan, *Nano Lett.*, 2008, **8**, 3858–3864.
17 C. Ma, D. Moore, J. Li and Z. L. Wang, *Adv. Mater.*, 2003, **15**, 228–231.
18 X. Zhou, C. Liu, L. Jiang and J. Li, *Colloids Surf., A*, 2004, **248**, 43–45.
19 L. Qi, *Coord. Chem. Rev.*, 2010, **254**, 1054–1071.
20 M. Li, H. Schnablegger and S. Mann, *Nature*, 1999, **402**, 393–395.
21 S. Acharya, I. Patla, J. Kost, S. Efrima and Y. Golan, *J. Am. Chem. Soc.*, 2006, **128**, 9294–9295.
22 S. Efrima and N. Pradhan, *C. R. Chim.*, 2003, **6**, 1035–1045.
23 A. B. Panda, S. Acharya and S. Efrima, *Adv. Mater.*, 2005, **17**, 2471–2474.
24 A. B. Panda, S. Acharya, S. Efrima and Y. Golan, *Langmuir*, 2007, **23**, 765–770.
25 N. Pradhan and S. Efrima, *J. Am. Chem. Soc.*, 2003, **125**, 2050–2051.
26 N. Pradhan and S. Efrima, *J. Phys. Chem. B*, 2004, **108**, 11964–11970.
27 N. Pradhan, B. Katz and S. Efrima, *J. Phys. Chem. B*, 2003, **107**, 13843–13854.
28 N. Belman, J. N. Israelachvili, Y. Li, C. R. Safinya, J. Bernstein and Y. Golan, *Nano Lett.*, 2009, **9**, 2088–2093.
29 F. Dumestre, B. Chaudret, C. Amiens, M.-C. Fromen, M.-J. Casanove, P. Renaud and P. Zurcher, *Angew. Chem., Int. Ed.*, 2002, **41**, 4286–4289.
30 X. Wang, J. Zhuang, Q. Peng and Y. Li, *Adv. Mater.*, 2006, **18**, 2031–2034.
31 S. Acharya, A. B. Panda, N. Belman, S. Efrima and Y. Golan, *Adv. Mater.*, 2006, **18**, 210–213.
32 M. George and R. G. Weiss, *J. Am. Chem. Soc.*, 2001, **123**, 10393–10394.
33 M. George and R. G. Weiss, *Langmuir*, 2002, **18**, 7124–7135.
34 M. George and R. G. Weiss, *Langmuir*, 2003, **19**, 1017–1025.
35 T. Holas, J. Zbytovska, K. Vavrova, P. Berka, M. Madlova, J. Klimentova and A. Hrabalek, *Thermochim. Acta*, 2006, **441**, 116–123.
36 N. Belman, J. N. Israelachvili, Y. Li, C. R. Safinya, J. Bernstein and Y. Golan, *J. Am. Chem. Soc.*, 2009, **131**, 9107–9113.
37 JCPDS, Powder diffraction file # 36–1450.
38 T. Ghoshal, S. Kar and S. Chaudhuri, *J. Cryst. Growth*, 2006, **293**, 438–446.
39 A. S. Akhmatov, *Molecular Physics of Boundary Friction*, Israel Program for Scientific Translations, Jerusalem, 1966.

SUPPLEMENTARY INFORMATION

Hierarchical Superstructure of Alkylamine-Coated ZnS Nanoparticle Assemblies

Nataly Belman,[a,b] Jacob N. Israelachvili,[c,d] Youli Li,[d] Cyrus R. Safinya,[e] Vladimir Ezersky,[a] Alexander Rabkin,[a,b] *O*lga Sima[a,b] *and* Yuval Golan[*a,b]

[a] *Department of Materials Engineering, Ben-Gurion University of the Negev, Beer-Sheva 84105, Israel. . Fax: +972-8-6472944; Tel: +972-8-6461474; E-mail: ygolan@bgu.ac.il*
[b] *Ilse Katz Institute for Nanoscale Science and Technology, Ben-Gurion University of the Negev, Beer-Sheva 84105, Israel*
[c] *Department of Chemical Engineering, and Materials Department, University of California, Santa Barbara, CA 93106, USA*
d. Materials Research Laboratory, University of California, Santa Barbara, CA 93106, USA
[e] *Materials, Physics, and Molecular, Cellular, and Developmental Biology Departments, University of California, Santa Barbara, CA 93106, USA*

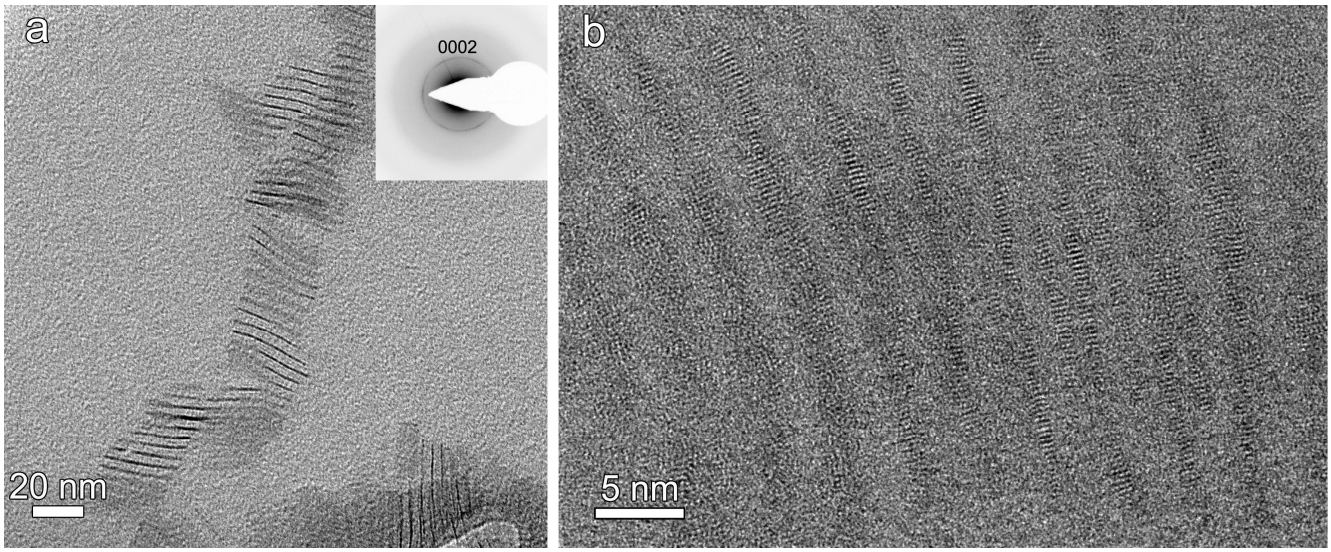

Figure S1. (a) BF TEM image and ED pattern (inset) of ODA-coated ZnS nanowires. (b) HRTEM image of ZnS nanowires. The nanowires were synthesized *using pure ODA surfactant* (not exposed to CO_2) under the same synthesis conditions (temperature and duration) as described in the Experimental Section for nanorod formation.

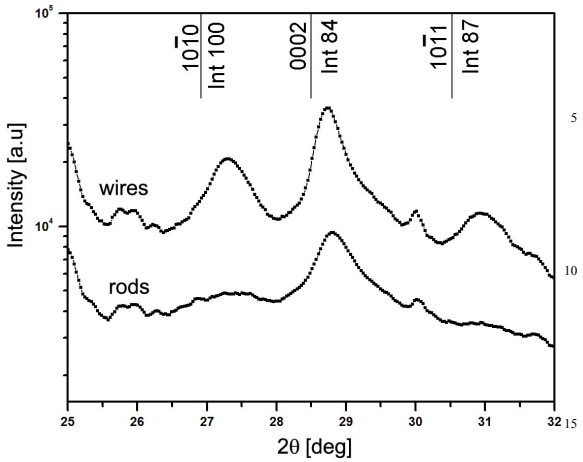

Figure S2. A part of powder XRD patterns of ODA-coated ZnS nanorods and nanowires (Figure 2a) and the expected peak positions and intensities of wurtzite ZnS based on JCPDS # 36-1450.

Diffraction Data Tables

Below we present diffraction data tables for the different nanoparticle morphologies described in the main text, including peak position in 2θ and corresponding d-spacings for (h k) planes calculated from the unit cell lattice constants (see Table 1 in main text). Peak positions observed experimentally in the diffractograms are marked in **bold**. X-ray source in all cases was Cu K_α (λ=1.54 Å).

Table S2. Crystallographic data for ODA-coated wires and rods corresponding to the diffractograms shown in Fig. 2a.

ODA-coated wires			ODA-coated rods		
(h k)	2θ [deg]	*d* [Å]	*(h k)*	2θ [deg]	*d* [Å]
(1 0)	**1.63**	**54.04**	**(1 0)**	**1.61**	**54.75**
(0 1)	**1.86**	**47.5**	**(0 1)**	**1.86**	**47.49**
(1 1)	2.47	35.677	(1 1)	2.46	35.875
(2 0)	**3.27**	**27.02**	**(2 0)**	**3.22**	**27.375**
(0 2)	**3.72**	**23.75**	**(0 2)**	**3.72**	**23.745**
(2 1)	3.76	23.486	(2 1)	3.72	23.717
(1 2)	4.06	21.743	(1 2)	4.05	21.785
(3 0)	**4.9**	**18.013**	**(3 0)**	**4.84**	**18.25**
(2 2)	4.95	17.838	(2 2)	4.92	17.937
(3 1)	5.24	16.843	(3 1)	5.18	17.035
(0 3)	**5.58**	**15.833**	**(0 3)**	**5.58**	**15.83**
(1 3)	5.81	15.195	(1 3)	5.81	15.207
(3 2)	6.15	14.352	(3 2)	6.1	14.47
(2 3)	6.46	13.661	(2 3)	6.44	13.704
(4 0)	**6.54**	**13.51**	**(4 0)**	**6.45**	**13.688**
(4 1)	6.8	12.995	(4 1)	6.72	13.152
(3 3)	7.43	11.892	(3 3)	7.39	11.958
(0 4)	**7.44**	**11.875**	**(0 4)**	**7.44**	**11.873**
(4 2)	7.52	11.743	(4 2)	7.45	11.858
(1 4)	7.62	11.598	(1 4)	7.61	11.603
(2 4)	8.13	10.871	**(5 0)**	**8.07**	**10.95**
(5 0)	**8.17**	**10.808**	(2 4)	8.11	10.892
(5 1)	8.38	10.539	(5 1)	8.28	10.67
(4 3)	8.6	10.277	(4 3)	8.53	10.354
(3 4)	8.91	9.914	(3 4)	8.88	9.952
(5 2)	8.98	9.837	(5 2)	8.89	9.944
(0 5)	**9.3**	**9.5**	**(0 5)**	**9.3**	**9.498**
(1 5)	9.44	9.357	(1 5)	9.44	9.358
(6 0)	9.81	9.007	(6 0)	9.68	9.125
(2 5)	9.86	8.962	(5 3)	9.81	9.005
(5 3)	9.9	8.927	(2 5)	9.85	8.973
(4 4)	9.91	8.919	(4 4)	9.85	8.969
(6 1)	9.99	8.849	(6 1)	9.86	8.961
(6 2)	10.5	8.421	(6 2)	10.38	8.518
(3 5)	10.52	8.403	(3 5)	10.49	8.425
(5 4)	11.06	7.993	(5 4)	10.98	8.049
(0 6)	**11.17**	**7.917**	**(0 6)**	**11.17**	**7.915**
(1 6)	11.29	7.833	(6 3)	11.18	7.906
(6 3)	11.29	7.829	(1 6)	11.29	7.834
(4 5)	11.38	7.771	(7 0)	11.3	7.821
(7 0)	11.45	7.72	(4 5)	11.33	7.803
(7 1)	11.6	7.62	(7 1)	11.46	7.717
(2 6)	11.64	7.597	(2 6)	11.63	7.604
(7 2)	12.04	7.342	(7 2)	11.9	7.429
(3 6)	12.2	7.248	(3 6)	12.18	7.262
(6 4)	12.32	7.176	(6 4)	12.22	7.235
(5 5)	12.39	7.135	(5 5)	12.33	7.175
(7 3)	12.75	6.939	(7 3)	12.61	7.012
(4 6)	12.95	6.83	(4 6)	12.91	6.852
(0 7)	**13.04**	**6.786**	(8 0)	12.92	6.844
(8 0)	13.1	6.755	**(0 7)**	**13.04**	**6.784**
(1 7)	13.14	6.733	(8 1)	13.06	6.774
(8 1)	13.23	6.688	(1 7)	13.14	6.733
(2 7)	13.44	6.581	(2 7)	13.43	6.585
(6 5)	13.54	6.536	(6 5)	13.44	6.58
(8 2)	13.62	6.497	(8 2)	13.45	6.576
(7 4)	13.67	6.472	(7 4)	13.55	6.532
(5 6)	13.85	6.387	(5 6)	13.79	6.415
(3 7)	13.93	6.35	(3 7)	13.91	6.359
(8 3)	14.24	6.213	(8 3)	14.09	6.282
(4 7)	14.6	6.064	(9 0)	14.55	6.083
(9 0)	14.74	6.004	(4 7)	14.56	6.079
(7 5)	14.77	5.991	(7 5)	14.66	6.038
(9 1)	14.86	5.957	(9 1)	14.67	6.034
(6 6)	14.89	5.946	(6 6)	14.8	5.979
(0 8)	14.91	5.938	**(0 8)**	**14.91**	**5.936**

(1 8)	15	5.902	(8 4)	14.93	5.929
(8 4)	15.08	5.872	(1 8)	15	5.902
(9 2)	15.21	5.821	(9 2)	15.02	5.893
(2 8)	15.27	5.799	(2 8)	15.26	5.801
(5 7)	15.41	5.747	(5 7)	15.35	5.767
(3 8)	15.7	5.639	(9 3)	15.59	5.678
(9 3)	15.77	5.614	(3 8)	15.68	5.645
(7 6)	16.02	5.527	(7 6)	15.92	5.563
(8 5)	16.09	5.505	(8 5)	15.95	5.553
(4 8)	16.29	5.436	(10 0)	16.18	5.475
(6 7)	16.34	5.42	(4 8)	16.26	5.446
(10 0)	16.39	5.404	(6 7)	16.27	5.444
(10 1)	16.5	5.369	(10 1)	16.28	5.439
(9 4)	16.53	5.358	(9 4)	16.36	5.414
(0 9)	**16.78**	**5.278**	(10 2)	16.6	5.335
			(0 9)	**16.79**	**5.277**

Table S2. Crystallographic data for ODA molecules adsorbed on ZnS nanoparticle surface as derived from powder XRD measurements (Fig. 2a).

	(*hk*)	2θ [deg]	*d* [Å]
ODA-coated wires	$(1\bar{1})$	18.92	4.68
	(01)	19.29	4.60
	(10)	19.83	4.47
ODA-coated rods	$(1\bar{1})$	18.95	4.68
	(01)	19.30	4.59
	(10)	19.85	4.47